sponds to an uncertainty of a satellite diameter in radial position, the upper band determined by considering a dipole tilt only while the lower band represents possible dipole tilt solutions when the effects of Saturn's ring current are considered. For the latter solution, field lines must be traced numerically from Voyager 2 to the equator. The Voyager 1 model of Saturn's ring current has been assumed in this example for demonstration purposes, although it is clear from the preceding discussion that the ring current and hence the nondipolar character of the field geometry may have been significantly changed at the time Voyager 2 encountered the Tethys L shell outbound. Both solutions demonstrate insensitivity to a rotation of the dipole tilt about the Saturn-spacecraft vector (or a translation of the dipole perpendicular to the Saturn-spacecraft vector).

Additional constraints based on particle species identification, the relative longitude of Tethys and Voyager 2 at event time, and particle drifts due to field gradients and curvature may further constrain the range of possible solutions. Clearly additional microabsorption features at longitudes around 90° or 270° SLS would also further constrain the solution.

Ring plane crossing. Because of the special circumstances (*15, 16*) surrounding the crossing of the ring plane by Voyager 2, we have investigated the detailed 60-msec data during a 16-minute interval centered on the nominal crossing time at day 238, hour 0418, for evidence of any unusual anomalies, and the central 6 minutes of these data are plotted in Fig. 8. There are no sudden changes evident or quasi-periodic variations that could be associated with any mechanical motion of the magnetometer sensor or with any localized field perturbations or wave phenomena. The regular toggling of the individual components between adjacent digital values is readily evident because the magnetic field components changed gradually throughout this sample. Note the very expanded scale of the plots in this figure, where the field intensity is approximately 1100 nT, so that the quantization step size of the 12-bit A-D converter yields a ± 0.5-nT uncertainty. This is well above the intrinsic noise level of the sensors measured in flight, which is less than 0.006 nT RMS equivalent over the 8.3-Hz bandwidth.

We conclude that there is no evidence in these detailed data for any special event or events which would have disturbed either the assumed orientation of magnetometer sensors or the ambient field at the location. The sensitivity is limited only by the quantization step size and the vector sample rate of 16⅔/second (Nyquist frequency = 8.33 Hz). The quantization limitation translates to an insensitivity to angular variations of less than 1.5 arc minutes. Short time scale events manifested as magnetic disturbances would be progressively attenuated by the instrument frequency roll-off characteristics beyond 5 Hz.

NORMAN F. NESS
MARIO H. ACUÑA
KENNETH W. BEHANNON
LEONARD F. BURLAGA
JOHN E. P. CONNERNEY
RONALD P. LEPPING
Laboratory for Extraterrestrial Physics, Goddard Space Flight Center, Greenbelt, Maryland 20771
FRITZ M. NEUBAUER
Technische Universität, Braunschweig, Federal Republic of Germany

References and Notes

1. K. W. Behannon, M. H. Acuña, L. F. Burlaga, R. P. Lepping, N. F. Ness, F. M. Neubauer, *Space Sci. Rev.* **21**, 235 (1977).
2. N. F. Ness, M. H. Acuña, R. P. Lepping, J. E. P. Connerney, K. W. Behannon, L. F. Burlaga, F. M. Neubauer, *Science* **212**, 211 (1981).
3. M. D. Desch and M. L. Kaiser, *Geophys. Res. Lett.* **8**, 253 (1981).
4. J. E. P. Connerney, M. H. Acuña, N. F. Ness, *Nature (London)* **292**, 724 (1981). The total current in the Voyager 1 model ring is ~ 7 × 10^6 A but was incorrectly given in this reference as 3 × 10^6.
5. N. F. Ness, M. H. Acuña, K. W. Behannon, F. M. Neubauer, *J. Geophys. Res.*, in press.
6. M. L. Kaiser *et al.*, *Nature (London)* **292**, 731 (1981).
7. G. L. Siscoe, L. Davis, Jr., P. J. Coleman, Jr., E. J. Smith, D. E. Jones, *ibid.* **73**, 61 (1968).
8. J. Y. Choe, D. B. Beard, E. C. Sullivan, *Planet. Space Sci.* **21**, 485 (1973).
9. E. J. Smith, L. Davis, Jr., D. E. Jones, P. J. Coleman, Jr., D. S. Colburn, P. Dyal, C. P. Sonett, *J. Geophys. Res.* **85**, 5655 (1980).
10. K. W. Behannon, J. E. P. Connerney, N. F. Ness, *Nature (London)* **292**, 753 (1981).
11. M. H. Acuña, J. E. P. Connerney, N. F. Ness, *ibid.*, p. 721.
12. J. E. P. Connerney, *J. Geophys. Res.* **86**, 7679 (1981).
13. R. E. Vogt, D. L. Chenette, A. C. Cummings, T. L. Garrard, E. C. Stone, A. W. Schardt, J. H. Trainor, N. Lal, F. B. McDonald, *Science* **212**, 231 (1981).
14. R. E. Vogt *et al.*, *ibid.* **215**, 577 (1982).
15. J. W. Warwick *et al.*, *ibid.*, p. 583.
16. F. L. Scarf, D. A. Gurnett, W. S. Kurth, R. L. Poynter, *ibid.*, p. 587.
17. J. H. Wolfe, J. D. Mihalov, H. R. Collard, D. D. McKibbin, L. A. Frank, D. S. Intriligator, *ibid.* **207**, 403 (1980).
18. We acknowledge useful discussions of these results with our Voyager colleagues and appreciate the expert assistance of our fellow Laboratory of Experimental Physics computer support staff under the able guidance of W. H. Mish. Finally, the attention given to supporting our experiment by the Jet Propulsion Laboratory staff is recognized and greatly appreciated. One of us, F.M.N., was supported financially by the German Ministry of Science and Technology.

10 November 1981

Plasma Observations Near Saturn: Initial Results from Voyager 2

Abstract. *Results of measurements of plasma electrons and positive ions made during the Voyager 2 encounter with Saturn have been combined with measurements from Voyager 1 and Pioneer 11 to define more clearly the configuration of plasma in the Saturnian magnetosphere. The general morphology is well represented by four regions: (i) the shocked solar wind plasma in the magnetosheath, observed between about 30 and 22 Saturn radii* (R_S) *near the noon meridian; (ii) a variable density region between* ~ *17* R_S *and the magnetopause; (iii) an extended thick plasma sheet between* ~ *17 and* ~ *7* R_S *symmetrical with respect to Saturn's equatorial plane and rotation axis; and (iv) an inner plasma torus that probably originates from local sources and extends inward from* L ≈ *7 to less than* L ≈ *2.7* (L *is the magnetic shell parameter). In general, the heavy ions, probably* O^+, *are more closely confined to the equatorial plane than* H^+, *so that the ratio of heavy to light ions varies along the trajectory according to the distance of the spacecraft from the equatorial plane. The general configuration of the plasma sheet at Saturn found by Voyager 1 is confirmed, with some notable differences and additions. The "extended plasma sheet," observed between* L ≈ *7 and* L ≈ *15 by Voyager 1 is considerably thicker as observed by Voyager 2. Inward of* L ≈ *4, the plasma sheet collapses to a thin region about the equatorial plane. At the ring plane crossing,* L ≈ *2.7, the observations are consistent with a density of* O^+ *of* ~ *100 per cubic centimeter, with a temperature of* ~ *10 electron volts. The location of the bow shock and magnetopause crossings were consistent with those previously observed. The entire magnetosphere was larger during the outbound passage of Voyager 2 than had been previously observed; however, a magnetosphere of this size or larger is expected* ~ *3 percent of the time.*

Before the Voyager 2 encounter with Saturn, our knowledge of the Saturnian magnetosphere was based on the results of the Pioneer 11 (*1*) and Voyager 1 (*2*) flybys. Since the inbound trajectories of Pioneer 11 and Voyager 1 were close to the noon meridian and to the equatorial plane of Saturn, measurements could be made only for a limited range of latitudes. The Voyager 2 trajectory traversed a significantly wider range in latitude and, as a result, the Voyager 2 experiments have provided new information about the spatial distribution and properties of charged particles in the magnetosphere of Saturn. The plasma experiment and methods of data analysis have been described (*3, 4*). We discuss here (i) the bow shock and magnetopause crossings, (ii) magnetospheric plasma observations, (iii) the characteristics and composition of the positive ions in the dayside outer magnetosphere, (iv) observations in the inner plasma torus, (v) general implications related to sources of plasma, and (vi) the interaction between the magnetospheric plasma and the neutral hydrogen cloud. Possible explanations for the significant differences between plasma observations at Saturn obtained from the Pioneer 11, Voyager 1, and Voyager 2 spacecraft are discussed.

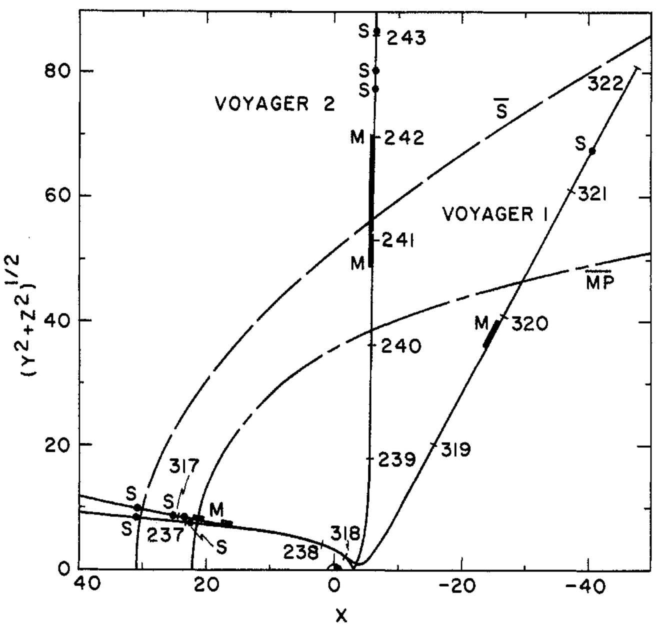

Fig. 1. Comparison of boundary locations observed by Voyager 1 and Voyager 2. The trajectories are shown in cylindrical coordinates with the Sun-Saturn line as the axis of the cylinder; average shock ($\bar{S}$) and magnetopause ($\overline{MP}$) shapes are scaled from the terrestrial boundaries. The portions of each trajectory between the first and last magnetopause crossings are indicated with a heavy line labeled *M*; the bow shock crossings are labeled *S*.

Table 1. Bow shock and magnetopause crossing.

Boundary	Day	Time	Distance	Predicted distance
		Inbound		
Shock	24 August (236)	1338	31.6	29.6 ± 0.3
		1708	29.0	27.8 ± 0.5
		1831	28.0	27.8 ± 0.9
		2020	26.6	23.4 ± 0.2
	25 August (237)	0026	23.6	24.7 ± 0.1
Magnetopause		0703	18.5	
		Outbound		
	28 August (240)	1620 to 1626		
		1644		
		1648		
		1650		
		1652 to 1700	48.6	
		1743 to 1809	49.1	
		2138		
		2148		
		2156	52.0	
		2255	52.7	
	29 August (241)	0421 to 0453	56.9	
		0620	57.9	
		0721	58.5	
		1620	64.8	
		1641	65.1	
		1814 to 1833	66.3	
	30 August (242)	0031	70.4	
Shock		1056	77.5	72.8 ± 6.7
		1121*		71.3 ± 8.2
		1129*		73.4 ± 0.0
		1407	79.5	75.2 ± 3.9
		1945	83.4	70.0 ± 4.3
	31 August (243)	0002	86.3	73.9 ± 2.6
		0108	87.0	67.0 ± 2.4

*The existence of these two shock crossings is uncertain.

Shock and magnetopause crossings. As Voyager 2 approached Saturn, the bow shock was crossed five times, but the magnetopause only once. Outbound, there were at least 17 crossings of the magnetopause and at least five of the bow shock, and the boundaries observed by Voyager 2 were farther from Saturn than those observed by Voyager 1 or Pioneer 11. A preliminary list of the bow shock and magnetopause crossings observed by Voyager 2 is given in Table 1; this list should be complete for all crossings that are more than 3 minutes apart. A corresponding list has been published for Voyager 1 (*2*). The locations of the boundary crossings observed by Voyager 1 and Voyager 2 are shown in Fig. 1 relative to "average" bow shock and magnetopause boundaries. These boundaries were obtained by scaling average terrestrial boundary shapes (*5*) to an average distance of shock to planet (based on 9 months of solar wind data extrapolated to Saturn) and assuming that the shock to planet distance varies as the inverse one-sixth power of the ram pressure, *P*, of the solar wind (*6*). As with Voyager 1, the position of the initial bow shock crossing observed by Voyager 2 closely agreed with that expected on the basis of the external ram pressure observed in the solar wind just before the time of the observed shock crossing; however, the boundaries on the outbound pass were much farther out than anticipated. Solar wind observations for the preceding 9 months indicated that the magnetosphere was this extended only ~ 3 percent of the time. Since February 1981, Voyager 2 has repeatedly encountered the Jovian wake and tail, which must presumably also have swept over the Saturnian magnetosphere (*7, 8*). Such an encounter with the Jovian wake and tail may have occurred during the outbound pass. Large amplitude waves on the boundary are probably required to explain the multiple magnetopause crossings.

Magnetospheric plasma observations. Data obtained by Pioneer 11 and Voyager 1 had been used to develop a model of the spatial distribution of plasma in the magnetosphere (*2*). The model consisted of an equatorially confined plasma sheet assumed to be symmetrical about the equator and rotation axis of Saturn. In the outer part of the sheet, at values of *L* between ~ 15 and ~ 7, plasma densities were nearly independent of *Z* and the thickness of the sheet was found to be ± 1.8 Saturn radii (R_S). (L is the equatorial distance of a magnetic field line and Z is the distance from the equatorial plane, both measured in R_S units.) In the inner sheet at values of L between ~ 7 and 4, the density profile was well fitted by a Gaussian distribution with a root-mean-square width of 0.9 R_S. These results are shown in the lower panel of Fig. 2, which also shows the trajectories of the three spacecraft—Pioneer 11, Voyager 1, and Voyager 2.

In general, the properties of the plasma, including number density, velocity, and composition, are functions of L and Z, and our objective is to describe the properties of the plasma sheet in those terms. Thus, construction of a reasonably representative model requires data over a wide range of L and Z for an extended period. It is apparent from Fig. 2, however, that the data set from any one spacecraft provides an extremely limited coverage of L-Z space and that an observed change in density or other parameter can be interpreted in terms of a dependence on L or Z or any combination of the two variables. For even a minimally complete data set, it is necessary to combine data from all three spacecraft under the assumptions of mirror and azimuthal symmetry (*9*). It is implicit in this procedure that temporal changes in the magnetosphere between or during the various encounters were small.

A cursory inspection of Fig. 2 shows that the trajectories of the three spacecraft were very different. Pioneer 11 inbound was close to the equatorial plane; it explored a large range in L, but a small range in Z. Voyager 1 inbound and outbound to $L \approx 11$ was limited to $Z \lessapprox 2.2$. Only Voyager 2 reached values of $|Z|$ that exceeded 2 R_S for all values of L greater than 5. The trajectory of Voyager 2 lay almost completely outside the location of the plasma sheet as deduced from Pioneer 1 and Voyager 1 data. The inbound trajectories of Voyager 1 and Voyager 2 almost coincided between $L \approx 4.5$ and $L \approx 5.7$; during this interval, the local times for the two spacecraft were nearly identical, so that the data sets should be directly comparable.

For reasons discussed in our account of the Voyager 1 flyby of Saturn (*2*), the spatial profile of low-energy magnetospheric plasma is more easily inferred from electron observations than from positive ion observations. Figure 3 displays the Voyager 2 measurements of plasma electron density [obtained by the method described in (*2*) and (*10*)] along the spacecraft trajectory, plotted in a

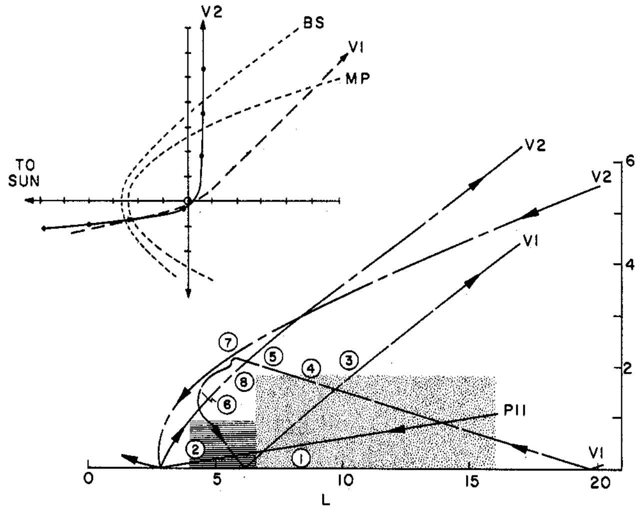

Fig. 2. The upper panel shows the Voyager 1 and Voyager 2 trajectories projected onto the orbital plane of Saturn and the positions of the bow shock and magnetopause observed by Voyager 1 (see text). The lower panel shows the Voyager 1, Voyager 2, and Pioneer 11 trajectories in a meridional plane folded about the equator; the curvilinear coordinate system is defined by the dipole shell parameter L and by the absolute distance from the spin equator, $|Z|$. Also shown is a schematic representation of the inner plasma torus and the extended plasma sheet. Circled numbers are used to identify particular points on the trajectories referenced in the text.

cylindrical, Saturn-centered coordinate system aligned with Saturn's rotation axis. The principal features of the density profile are (i) the decrease of electron density associated with the inbound crossing of the magnetopause at 18 R_S; (ii) a region of relatively low, highly variable densities on the inbound pass between the magnetopause and 11 R_S, and again on the outbound pass beyond 16 R_S; (iii) a steady increase of density with decreasing radial distance both on the inbound pass (11 to 4 R_S) and on the outbound pass (4 to 16 R_S), which delineates the plasma sheet surrounding Saturn; (iv) an apparent decrease of density to very low values with decreasing radial distance at 4 R_S, both inbound and outbound. In reality the apparent decrease in density inside ~ 4 R_S is an artifact of the data reduction; it results not from a real decrease in plasma density but from

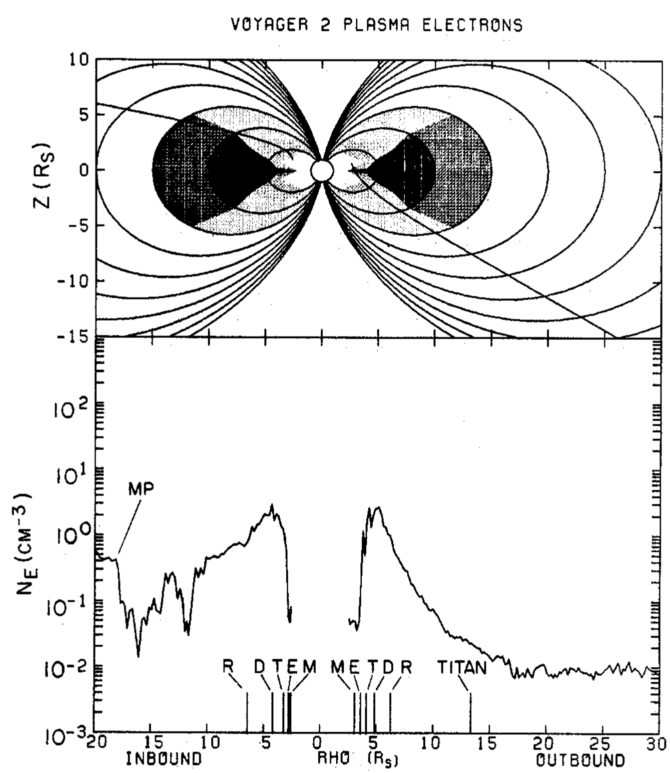

Fig. 3. The lower panel shows 15-minute averages of plasma electron densities (per cubic centimeter) plotted against ρ, the perpendicular distance from Saturn's rotation axis. The inbound pass from the last magnetopause crossing is plotted from the left with the outbound pass to ρ = 30 on the right; thus time increases monotonically along the abscissa. Values of ρ at which the spacecraft crossed the L shells of Titan, Rhea (R), Dione (D), Tethys (T), Enceladus (E), and Mimas (M) are indicated above the abscissa. The upper panel shows the spacecraft position in the same coordinate system; Z is the distance from the equatorial plane. Dipolar field lines corresponding to indicated values of the flux tube parameter L are also shown. The shaded regions represent a qualitative picture of the plasma morphology inside 15 R_S. The vertical extent of the sheet has been determined from scale heights calculated from electron temperatures as described in the text. The darker region refers to a plasma containing only O^+ and electrons, and the lighter region to one containing protons and electrons.

a rapid decrease in electron temperature at $L \approx 4$. Thus, inside $\sim 4\ R_S$ the electron data do not provide useful measurements of the density. However, some information can be obtained from the positive ion data; these results inside 4 R_S are considered in detail in a subsequent section.

The configuration of the plasma sheet suggested by the data in Fig. 3 is characterized by a considerable thickness, and in contrast to the Voyager 1 results, relatively high electron densities associated with the plasma sheet are observed at distances from the equatorial plane as large as ~ 4 or 5 R_S. Evidently, either the magnetosphere of Saturn changed significantly between the Voyager 1 and Voyager 2 flybys or some of the assumptions of the Voyager 1 analysis [in (2)] (for example, azimuthal symmetry) were inappropriate, or both.

Instead of using the actual electron densities plotted in Fig. 3 it is instructive to adopt a variable obtained by multiplying the actual densities by a suitable power of L. This procedure compensates for the large systematic increase in density with decreasing radial distance and yields a variable that better represents the dependences of the model on Z and L. In the Voyager 1 analysis (2) n_eL^3 was used as the appropriate variable, both on theoretical grounds related to flux tube content (11) and on empirical evidence of near constancy over large segments of the trajectory. For Voyager 2, the systematic increase of n_e with decreasing distance is observed over a slightly wider range of L than was the case for Voyager 1, and n_eL^4 proves to be more nearly constant than n_eL^3; accordingly, we use n_eL^4 instead of n_eL^3 in further analysis (the use of n_eL^3 for Voyager 2 or n_eL^4 for Voyager 1 leads to substantially the same conclusions). The dominant feature of Voyager 2 observations is a sharp decrease of n_eL^4 observed inside of points 7 and 8 in Fig. 2. These points identify a region in which n_eL^4 decreases with decreasing L or $|Z|$ relative to the nearly constant values at larger L or $|Z|$. Figure 4 shows n_eL^4 in the vicinity of the decrease as a function of L and as a function of $|Z|$; it is apparent that the plot against L gives much better agreement between inbound and outbound passes. Therefore, we interpret the decrease observed at points 7 and 8 in Fig. 2 in terms of a dependence primarily on L rather than on $|Z|$. Thus, the Voyager 2 observations show that the extended plasma sheet has a thickness that exceeds the range of the observations (up to values of $|Z|$ between ~ 4 and 5) and has a sharp inner boundary at $L \approx 6$.

The complete radial profile of n_eL^4 for Voyager 2 out to $L \approx 14$ is given in Fig. 5. The pattern described above is clearly apparent—a nearly constant $n_eL^4 \approx 5.5 \times 10^3$ cm^{-3} for $L > 6$ and a sharp decrease inside $L \approx 6$, with a slope of nearly a decade per R_S. Also shown for comparison in Fig. 5 are the Voyager 1 observations; the profile of n_eL^4 during the inbound pass is almost identical with the Voyager 2 results—a nearly constant average level at the same value of $n_eL^4 \approx 5.5 \times 10^3$ cm^{-3} for large values of L and a sharp decrease for smaller values of L, the sole difference being that the decrease sets in at $L \approx 8$ instead of at $L \approx 6$. (The larger values near closest approach and near the beginning of the outbound pass of Voyager 1 are associated with the passage of the spacecraft through the distinct spatial region of the inner plasma torus.) In our original interpretation of the Voyager 1 observations, we assumed that point 4 in Fig. 2 was associated with a passage through a thickness boundary and point 5 through a radial boundary. We now suggest that the overall decrease at points 4 and 5 represents passage through a single radial boundary, analogous to points 7 and 8 for Voyager 2, but located at $L \approx 8$

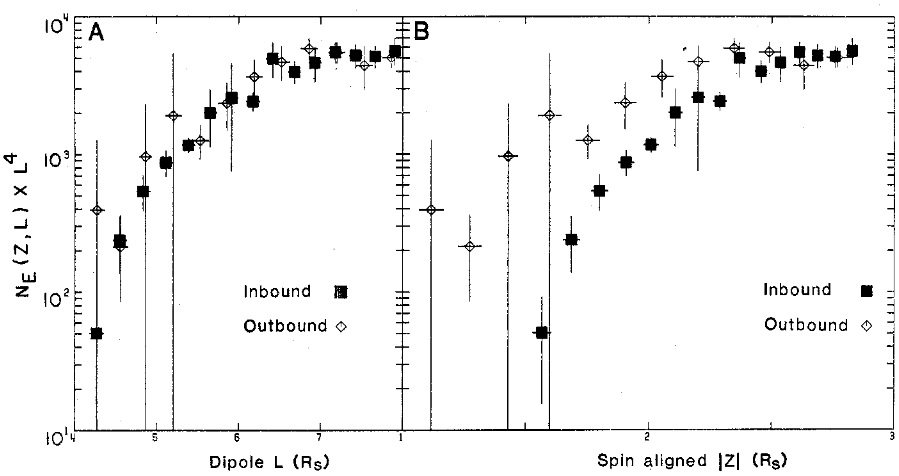

Fig. 4. Analysis of the plasma electron data from Voyager 2 in terms of L shell and distance, $|Z|$, from the equatorial plane. Only data for $4 < L < 8$ are used; each point represents a 15-minute average of electron measurements. Gross radial variations are removed by plotting n_eL^4 against L in (A) and against $|Z|$ in (B). The error bars were computed from the extremal values of n_e and L during the 15-minute averaging period.

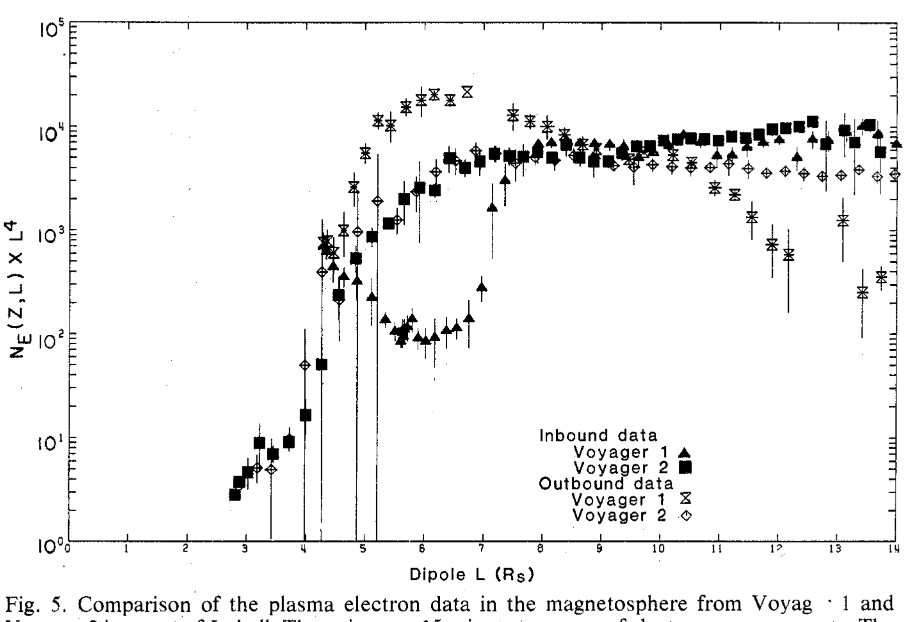

Fig. 5. Comparison of the plasma electron data in the magnetosphere from Voyager 1 and Voyager 2 in terms of L shell. The points are 15-minute averages of electron measurements. The error bars were computed from the extremal values of n_e and L during the 15-minute averaging period.

instead of $L \approx 6$. With this interpretation, the decrease of $n_e L^4$ at $L > 10$ on the Voyager 1 outbound pass remains the sole evidence for a limited thickness of the extended plasma sheet.

This conclusion—that the extended plasma sheet observed in the dayside magnetosphere at the time of the Voyager 1 encounter might have had a considerable thickness (as was observed by Voyager 2)—is strengthened by estimates of the scale height of the plasma sheet obtained from systematic measurements of electron temperatures during both encounters. An exact calculation requires knowledge of the plasma composition, the temperatures of the ions and electrons, and the pitch angle distributions. For our purposes, however, a rather crude estimate for a single ion component plasma (O^+ or H^+) is sufficient. We used 15-minute averages of the electron temperature measurements, assumed temperature equilibrium between ions and electrons, and assumed an isotropic Maxwellian distribution to derive corresponding estimates of the scale height, H, along the trajectories of both Voyager 1 and Voyager 2. The results provide additional information about the configuration of the plasma sheet as observed by the two spacecraft.

Inbound, both Voyager 1 and Voyager 2 observed a gradual decrease in proton scale height from $H \approx 10\ R_S$ at $L = 9$ to $H \approx 2\ R_S$ at $L = 4.5$. In this region, the scale heights observed by the two spacecraft are virtually indistinguishable. It is apparent from Fig. 5 that the values of $n_e L^4$ observed during the inbound pass of Voyager 1 in the region $L \approx 4.5$ to 7 fall markedly below the values observed on the outbound pass. During this interval of L on the outbound pass, Voyager 1 was close to the equatorial plane at a distance comparable to the scale height calculated for a single component O^+ plasma. On the other hand, during the inbound pass, the spacecraft was about two O^+ scale heights above the plane. Thus, it seems likely that the large difference in $n_e L^4$ observed during this interval can be attributed to the region of increased density expected near the equator for a multicomponent plasma of heavy and light positive ions. Confirmation of this result must await a more detailed ambipolar calculation. Beyond $L = 9$, values of H for both sets of data are in the range of $\sim$ 10 to $\sim$ 18 R_S, but those from Voyager 2 lie somewhat below those from Voyager 1. Thus from this evidence, the plasma sheet seen by Voyager 1 should have been slightly thicker than that seen by Voyager 2.

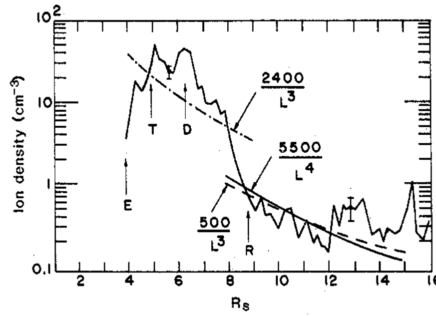

Fig. 6. Comparison between Pioneer 11 ion densities and the Voyager 1 and Voyager 2 plateau electron densities as a function of the planetocentric radial distance. E, T, and D are Enceladus, Tethys, and Dione.

In contrast to observations on the inbound trajectories of Voyager 1 and Voyager 2, there are large differences in the proton scale heights observed by the two spacecraft on the outbound trajectories. In particular, there is a large discontinuity in the Voyager 1 data outbound between $L \approx 10$ and $L \approx 16$. This region, in which the plasma electron densities drop to very low values and the electron temperatures increase markedly, appears to correspond exactly to "dropouts" in the charged particle counting rates reported by the cosmic-ray subsystem (CRS) and low-energy charged particle (LECP) experimenters (*12, 13*). Thus, although there is no obvious explanation for the effect, it seems clear that the data from Voyager 1 outbound show a strong apparent local time asymmetry beyond $L = 10$ that requires further investigation.

To summarize, the principal results from Voyager 2 and Voyager 1 concerning the configuration of the plasma sheet outside 4 R_S are the following.

1) The Voyager 2 observations are consistent with the Voyager 1 observations on the inbound trajectory except that the inner boundary of the extended sheet is found at about $L = 6$ instead of $L = 8$. Outbound, the observations of Voyager 2 show a thick plasma sheet out to $L \approx 17$. The Voyager 1 data agree out to $L = 10.5$; beyond that point the densities are anomalously low.

2) The Voyager 1 data show a gradual increase in $n_e L^3$, which begins after point 6 in Fig. 2 and was used to infer the thickness structure of the region, which in (*2*) was named the central plasma sheet; the radial boundaries of this region at $L \approx 4$ and $L \approx 7.5$ were inferred from Pioneer 11 observations at points 1 and 2 (*1*). We propose now that this region be called the inner plasma torus, which suggests more clearly the geometric structure and probable origin of the region. Although the trajectory of Voyager 2 was outside this region, the Voyager 2 observations do provide additional information concerning the inner boundary at $L \approx 4$ and the ion measurements roughly define the configuration of the torus between $L \approx 4$ and $L \approx 2.7$, as discussed below.

3) The density values observed inside the extended plasma sheet show remarkable agreement between Voyager 1 and Voyager 2, as well as with Pioneer 11. On the average, $n_e L^4$ is approximately constant ($\sim 5.5 \times 10^3$ cm^{-3}) and independent of Z within the boundaries of the plasma sheet as defined by observations from the respective spacecraft.

4) The apparent local time asymmetry observed by Voyager 1 outbound might be explained in a number of ways. We believe the most likely explanation is a time variation during the flyby. An increase in external solar wind pressure by about a factor of 2 was observed during the appropriate time interval by Voyager 2; this change provides a plausible mechanism for triggering a plasma loss from the magnetosphere (*6, 13a*).

Finally, in Fig. 6, the models of n_e inferred from Voyager 1 and Voyager 2 are compared with the ion density observations of Pioneer 11; the equatorial density profile deduced from the Voyager 1 model (*2*), together with the density implied by the constant level $n_e L^4 \approx 5.5 \times 10^4$ cm^{-3}, as shown superimposed on the radial profile published by Frank *et al.* (*1*). In the range of $L \approx 8.5$ to $L \approx 15$, the general trend of the Pioneer observations agrees well with the $n_e L^4$ or $n_e L^3$ dependence inferred from the Voyager analyses. The agreement of the absolute values is certainly as good as can be expected in view of the uncertain intercalibration of the two instruments and of the analyses. The higher densities derived from the Pioneer 11 observations between $L \approx 4$ and $L \approx 8$ are slightly larger than, but not grossly inconsistent with, the Voyager 1 model of the inner plasma torus.

Characteristics of the positive ions in the dayside magnetosphere. During its inbound traversal of the dayside magnetosphere, the Voyager 2 spacecraft had an orientation similar to that of Voyager 1, that is, with the side sensor of the plasma instrument facing nearly into the corotating magnetospheric flow. Figure 7 shows sequences of positive ion spectra obtained by the Voyager 1 and Voyager 2 side sensors inbound from ~ 18 to 14 R_S (*14*).

The spectra show clearly the large variations in the density and temperature

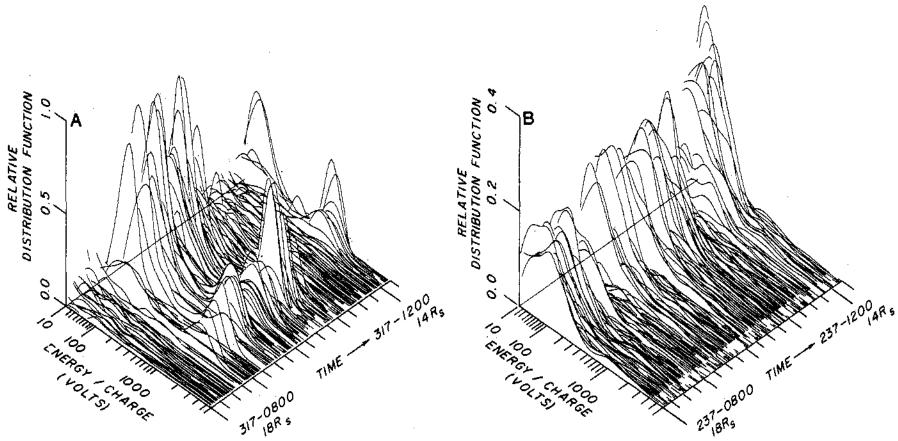

Fig. 7. Sequences of ion spectra from (A) Voyager 1 and (B) Voyager 2 between 18 and 14 R_S in the dayside magnetosphere. Values of the relative distribution function obtained from low-resolution mode spectral measurements made by the side-looking D sensor are plotted against energy per charge. The spectral points are interpolated by use of a cubic spline.

of the plasma ions in this region. The electron densities and temperatures show similar strong fluctuations; the electron density jumps frequently and abruptly by about one order of magnitude; the higher density value (accompanied by lower temperature) varies rather smoothly from 0.1 cm^{-3} near the magnetopause to 0.4 cm^{-3} at 11 R_S, inside of which the density begins to increase smoothly without frequent jumps. The lower value (and higher temperature) also varies rather smoothly from 6×10^{-3} cm^{-3} near the magnetopause to 2×10^{-2} at 11 R_S. Similar variations were seen in the Voyager 1 electron observations (*2*) at much lower latitudes. It appears that the spacecraft were alternately sampling two regions: a colder one with higher density and a hotter one with lower density. Similar regions were observed by both Voyagers in the front side magnetosphere of Jupiter (*15*), and it is known that detached plasma "islands" exist outside of Earth's plasmapause (*16*). Whether all of these features have the same generic origin remains to be seen. Two models of current interest are being considered in detail by our group (*17, 18*). The higher density regions may be detached plasma "blobs" from the denser region inside of ~ 11 R_S or they may be related to crossing Titan-released plasma plumes that extend downstream in the magnetospheric flow.

When the ions are sufficiently cold, distinct peaks can be resolved in the energy/charge spectra. Figure 7 shows clearly the similarities and differences between Voyager 1 and Voyager 2 observations. The dominant peak at low energies is consistent with that expected from protons rigidly corotating with Saturn; the second peak (evident in the Voyager 1 data) is consistent with heavier ions (such as O^+ or N^+) with the same bulk motion. For Voyager 2 data, the number of occasions for which the second peak could be clearly resolved were significantly fewer than they were for Voyager 1.

The proton densities derived from Voyager 2 spectra are less by a factor of ~ 3 than the densities measured at the same distance by Voyager 1. On the few occasions when the heavy ion peak is resolved in the Voyager 2 spectra, the ratio of the number of heavy ions to that of light ions appears to have decreased by a factor of ~ 20 in comparison with the Voyager 1 measurements at lower latitudes. The different ratios of heavy to light ions measured by the two spacecraft show that, as expected, the heavier ions are more closely confined in a region near the equatorial plane than the protons are.

In the absence of time variations in the interval between encounters, the change in the ratio of the number of heavy ions to that of light ions with distance from the equator shown by the Voyager 1 and Voyager 2 ion measurements can be interpreted in terms of a scale height for the ions. If temperature equilibrium is assumed, the ambient plasma temperature which corresponds to the scale height was ~ 150 eV, in agreement with direct measurements of electron temperatures. This temperature is considerably higher than that derived from some of the well-resolved spectra in Fig. 7. However, the few spectra that have been analyzed in detail were chosen because they have particularly well-resolved peaks and, hence, are probably associated with plasma that is cooler than the ambient plasma in that region.

Observations in the inner plasma torus. The existence of an inner plasma torus at Saturn was inferred from the results of Pioneer 11 (*1*) and Voyager 1 (*2*). This relatively dense equatorially confined plasma sheet extended inward from about $L = 7.5$ to at least $L = 4.5$. The location of the inner edge was not determined by the previous measurements because the corotating plasma fell below the energy/charge range of the Pioneer 11 plasma instrument at $L \approx 4.5$ and because the Voyager 1 trajectory crossed the upper boundary of the torus at $L \approx 4.5$.

The trajectory of Voyager 2 passed through the expected region of the inner torus inward of $L \approx 4.5$ and provided an opportunity to determine the characteristics of the plasma sheet to $L \approx 2.8$. As we remarked earlier, we derived the spatial distribution of plasma densities in the Saturnian magnetosphere from measurements of electron densities rather than of positive ion densities. Inside $L \approx 4.5$, the electrons become so cold that reliable measurements of n_e are no longer possible, a situation reminiscent of the cold inner Io plasma torus at Jupiter (*19*). Thus, for estimates of the plasma density, it is necessary to use the positive ion data in a region where the corotational flow is at large angles to viewing directions of all four sensors and in which the energy/charge of corotating H^+ and even O^+ falls below values that can be measured by straightforward methods. For these reasons, the analysis of data inward of ~ 4.5 R_S and the results discussed in this section must be regarded as preliminary.

Figure 8 shows the time sequence of positive ion spectra taken by the A sensor (*3*) during the time interval 0000 to 0816 of day 238—approximately centered on the ring plane crossing at $L = 2.73$. During this interval, the component of corotational flow into the A sensor varied between +10 and −40 km/sec. A corotating plasma beam can be detected only when the energy/charge of the component of particle velocity into the A sensor is above the 10-V threshold of the instrument. This will occur if there is a sufficient thermal spread to the beam even when the flow direction is not into the sensor.

At the beginning of day 238, the increasing currents in the low channels qualitatively followed the increasing electron density. Examination of these data suggests that these spectra represent the high-energy tails of Maxwellian proton distributions whose peaks have moved below the energy/charge threshold of the instrument as the spacecraft approached the planet. The presence of heavy ions in this region cannot be strictly ruled out, although if they were present, there must have been fewer of them than there were of protons. A preliminary analysis of the observations at 0127 of day 238 (L = 4.4) was made using data from the lowest four channels of the L mode, using data from all four sensors, and using the full response functions of the sensors. The results show clearly that these ions are protons with a density of 5 ± 1.5 cm^{-3} and a temperature of 8 ± 2 eV. The subsequent decrease of the measured ion currents at about 0130 corresponds roughly to the time of the decrease in electron temperature and to the apparent decrease in electron density.

This decrease in the observed currents at 0130 must reflect an abrupt change in the properties of the plasma ions, such as composition, temperature, or density; the decrease cannot be understood solely in terms of changes in corotation speed, spacecraft orientation, or instrument response to a corotating flow.

As the spacecraft approached the equatorial plane, the measured currents again increased, but this time much more strongly in the A sensor than in the others. A distinct signature is present from about 0340 to ~ 0440 as the spacecraft moved from ~ 0.42 R_S above the equatorial plane to 0.24 R_S below it (L shells between 2.73 and 3.05 were traversed in this period). During this period, well-measured currents were observed in at least three of the four sensors. Preliminary analysis of four spectral sets obtained during this period shows a qualitative difference from the set observed at 0127. Various fits indicate that the observed ions are O^+, although other species with mass-to-charge ratios greater than 1, for example, O^{+2} and $O_2{}^+$, cannot be conclusively ruled out by the present analysis.

A more detailed analysis of these four sets of spectra has been made under the assumptions of rigid corotation, a single ionic species, O^+, and an isotropic Maxwellian distribution. The observations were then fitted by varying the thermal speed and spacecraft potential over limited ranges of values and comparing the results with the actual data. Best agreement with the data is obtained for a temperature of ~ 10 eV (10 km/sec) and a spacecraft potential of a few volts. The ion density implied by this process varies strongly with both parameters; a peak density of O^+ in the range 50 to 150 cm^{-3} is indicated, the best value being ~ 100 cm^{-3}. The immediate interpretation of these data is that no sharp inward edge of the inner plasma torus exists at $L \approx 4.5$; this L shell simply marks the location of a steep thermal gradient. With respect to L values, the plasma population extends inward to at least 2.7 and possibly farther.

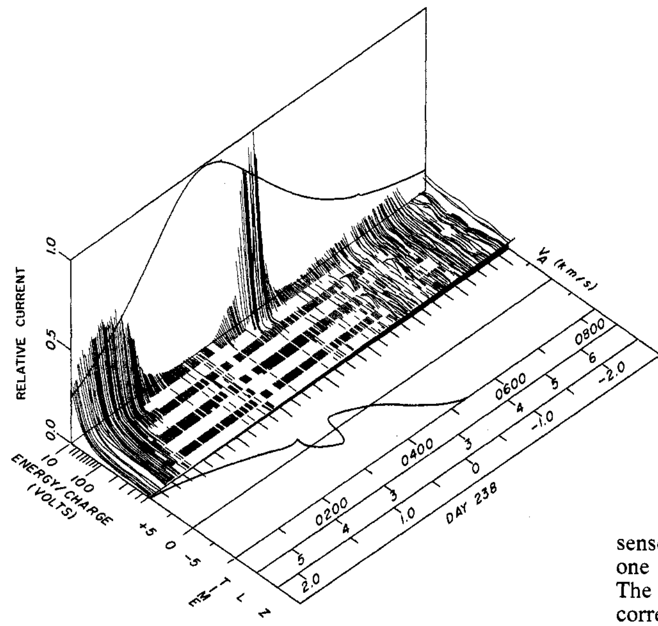

Fig. 8. Sequence of ion spectra taken from 0000 to 0816 on 26 August 1981. The relative currents obtained from low-resolution mode spectral measurements made by the A sensor are plotted against energy per charge. The spectral points are interpolated by use of a cubic spline fit. The magnitude of the Saturnian magnetic field at the position of the spacecraft is plotted on the back panel (*25*). The component of the corotation velocity (in the spacecraft frame) into the A sensor, V_A, is shown along one axis for the same period. The time of observation, the corresponding dipole L shell, and distance from the equator (Z in R_S) are also shown.

Quantitatively, a simple scale height model does not adequately describe the situation in this region. The actual variation in ion densities obtained near the crossing of the equatorial plane is consistent with a scale height of 0.2 R_S (for O^+). However, the O^+ temperatures derived from the fits are ~ 10 eV (about the same as those for the protons at 0127); this value corresponds to a scale height of 0.9 R_S. Since a scale height of 0.2 R_S corresponds to an O^+ temperature of 0.5 eV, the plasma is much too hot to be consistent with a simple scale height model of the density distribution. An appropriate anisotropy in the ion distribution function might account for this discrepancy, although this possibility has not yet been thoroughly investigated.

Any protons present at this time are apparently so cold that they cannot be measured. If the proton thermal speeds in this region were as low as 10 km/sec, the same as that for O^+, then the measured spectra would be consistent with a proton number density of no more than 200 cm^{-3} in addition to the ~ 100 cm^{-3} of O^+ ions that are directly measured.

Such large densities might be expected to be associated with various plasma wave emissions that were not observed at the ring plasma crossing. However, as indicated above, higher-energy plasma electrons with temperatures above ~ 30 eV are strongly depleted near the ring plane crossing. As a consequence, the population of suprathermal electrons, 1 to 30 keV, is inadequate to supply the resonant electrons necessary to produce the whistler chorus; upper hybrid resonance or gyroharmonic emissions are also unlikely because the usual phase-space free energy source is absent. Neither of these emissions have been observed by the plasma wave experimenters (*20*).

Implications for plasma sources. The source or sources of plasma for the various regions of Saturn's magnetosphere remain a major unresolved question. The inner plasma torus spatially overlaps Tethys, Dione, and the G and E rings; it also overlaps Enceladus and possibly extends as far inward as the A ring. All of these objects are therefore plausible sources of plasma for the inner torus; sputtering from ice-covered surfaces, as suggested by Frank *et al.* (*1*) is a likely mechanism.

On the basis of Voyager 1 data (*2*), the flux tube content of the inner torus at $L \approx 5$ and of the extended plasma sheet were found to be comparable. However, since the extended plasma sheet observed by Voyager 2 has approximately the same density at a given L, but a much larger thickness than the model derived from Voyager 1 data, it is clear now that the flux tube content in the extended plasma sheet significantly exceeds that of the inner torus. Hence, the plasma source for the extended plasma sheet cannot be the inner objects, as for the inner torus, but must be one or more of the following: the ionosphere of Saturn, ionization of the neutral hydrogen torus, or injection from Titan. The observed Voyager 2 profile of $n_e L^4$ (Figs. 4 and 5) is very similar to predictions based on an ionospheric diffusive source (*21*), which all have a sharp drop at $L \approx 7$ and a nearly constant level outside $L \approx 7$. However, it is rather difficult to explain in these models a change of the inner boundary from 6 R_S to 8 R_S without a change of magnitude.

Finally, there is the alternative possibility that the inner torus may have its source in the extended sheet; the two would then be related in the same way as the cold torus and the hot torus near Io in the magnetosphere of Jupiter (*22*). In this case, a cooling mechanism is required to play the same role as radiation does in the Jovian case; the possibility of cooling through absorption and reemission of electrons by E ring particles (*23*) may deserve further consideration.

Neutral hydrogen cloud. The Voyager 1 ultraviolet experimenters reported the discovery of a torus of neutral hydrogen extending from about 25 R_S inward to about 8 R_S. It was suggested by Broadfoot *et al.* (*24*) that the inner boundary occurs where it does as a result of ionization processes or charge exchange with plasma (or both). We show in what follows that this suggestion is consistent with the plasma data and that the same processes might determine the position of the outer boundary.

Figure 9 shows the lifetime against ionization of a neutral hydrogen atom in circular orbit around Saturn as a function of the radius of the orbit. Since Titan is the source of the neutral hydrogen torus, actual orbits are ellipses that cross the orbit of Titan. Thus, actual lifetimes must be found by an appropriately weighted average of the values shown in the figure. The calculated lifetimes take account of photoionization, electron impact ionization, and charge exchange. The plasma parameters used to determine the last two of these were values that typified the composite measurements of all three encounters.

The curve shows a decrease in the lifetime at locations corresponding to the observed inner and outer edges of the hydrogen torus. One can anticipate that the actual lifetimes based on elliptical orbits will be less at greater distances relative to the values at closer distances, because of the different exposure times

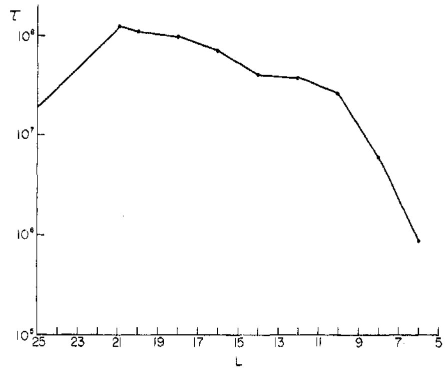

Fig. 9. The ionization lifetime, τ, for hydrogen as a function of L. The lifetime was computed by combining the rates for photoionization, electron impact ionization, and charge exchange with protons. The magnetospheric plasma parameters used to determine τ were representative values measured along the Voyager 1 and Voyager 2 trajectories. The magnetosheath parameters are based on an average density of 0.4 cm^{-3}, an electron temperature of 100 eV, and an average magnetopause position of 22 R_S. This position is based on a 9-month average of Voyager 1 solar wind data extrapolated to the position of Saturn.

to the plasma environment. Thus, the resemblance of the lifetime curve to the observed hydrogen torus should be improved by a more exact calculation.

H. S. BRIDGE
F. BAGENAL, J. W. BELCHER
A. J. LAZARUS, R. L. MCNUTT
J. D. SULLIVAN, P. R. GAZIS
Center for Space Research and *Department of Physics, Massachusetts Institute of Technology, Cambridge 02139*
R. E. HARTLE
Laboratory for Planetary Atmospheres, Goddard Space Flight Center, Greenbelt, Maryland 20771
K. W. OGILVIE
J. D. SCUDDER
E. C. SITTLER
Laboratory for Extraterrestrial Physics, Goddard Space Flight Center
A. EVIATAR*
G. L. SISCOE
Department of Atmospheric Sciences, University of California, Los Angeles 90024
C. K. GOERTZ†
Department of Physics and Astronomy, University of Iowa, Iowa City 52242
V. M. VASYLIUNAS
Max-Planck-Institut für Aeronomie, Katlenburg-Lindau, West Germany

References and Notes

1. L. A. Frank, B. G. Burek, K. L. Ackerson, J. H. Wolfe, J. D. Mihalov, *J. Geophys. Res.* **85**, 5695 (1980).
2. H. S. Bridge *et al.*, *Science* **212**, 217 (1981).
3. H. S. Bridge, J. W. Belcher, R. J. Butler, A. J. Lazarus, A. M. Mavretic, J. D. Sullivan, G. L. Siscoe, V. M. Vasyliunas, *Space Sci. Rev.* **21**, 259 (1977).
4. H. S. Bridge *et al.*, *Science* **204**, 987 (1979).
5. H. C. Howe and J. H. Binsack, *J. Geophys. Res.* **77**, 3334 (1972).
6. J. D. Sullivan, P. R. Gazis, H. S. Bridge, in preparation.
7. F. L. Scarf, W. S. Kurth, D. A. Gurnett, H. S. Bridge, J. D. Sullivan, *Nature (London)* **292**, 585 (1981).
8. S. Grzedzielski, W. Macek, P. Oberc, *ibid.*, p. 587.
9. We retain the assumption of reflection symmetry about the equatorial plane, since we consider a major north-south asymmetry of the magnetospheric plasma in the region of observation (L = 2) to be almost inconceivable; although asymmetries in the plasma sources can be readily imagined (for example, unequal illumination of the northern and southern ionospheres by sunlight, or a displacement of the dipole magnetic equator from the ring plane), the mirroring motion of plasma particles in the magnetic field imposes north-south symmetry unless the particles can be absorbed while crossing the ring plane with a high probability per single crossing (say, 30 to 50 percent); such a high probability would imply ring plane opacities of 0.3 to 0.5, in contrast to the estimated values of 10^{-6} and 10^{-7} [see H. J. Reitsema, B. A. Smith, S. M. Larson, *Bull. Am. Astron. Soc.* **12**, 701 (1980)].
10. J. D. Scudder, E. C. Sittler, H. S. Bridge, *J. Geophys. Res.* **86**, 8157 (1981).
11. The plasma content of a unit magnetic flux tube is proportional to either of the integrals, $\int dZ\, n_e L^3$ or $\int d(\cos O) n_e L^4$, where O is the colatitude.
12. R. E. Vogt *et al.*, *Science* **212**, 231 (1981).
13. S. M. Krimigis *et al.*, *ibid.*, p. 225.

13a. K. W. Behannon, J. E. P. Connerney, N. F. Ness, *Nature (London)* **292**, 753 (1981).

14. The Voyager 1 spectra shown in Fig. 7 were shown in figure 3 of (*2*), with the measured currents plotted as a function of energy/charge for each spectrum. The vertical axis in that figure was incorrectly labeled "relative distribution function," when it should have been "relative current." A 128-point cubic-spline fit was used instead of a 64-point fit.
15. Unpublished results of the plasma science experiment obtained during the Voyager 1 and Voyager 2 encounters with Jupiter.
16. C. R. Chappell, *J. Geophys. Res.* **79**, 1861 (1974).
17. A. Eviatar, G. L. Siscoe, J. D. Scudder, E. C. Sittler, Jr., J. D. Sullivan, in preparation.
18. C. K. Goertz, private communications.
19. Inside $L \approx 4$ the "apparent" electron number densities are two to three orders of magnitude less than the ion densities. This situation obtains because the electrons are cold, and most electrons have energies below the threshold of the first channel of the instrument (10 eV). An upper limit for the electron temperature in this region can be inferred from measurements of n_+/n_- (the ratio of the number of positive ions to that of electrons) and is $T_e \approx 1$ eV.
20. F. L. Scarf, D. A. Gurnett, W. S. Kurth, R. L. Poynter, *Science* **215**, 587 (1982).
21. G. L. Siscoe, in *Solar System Plasma Physics—A Twentieth Anniversary Review*, C. F. Kennel, L. J. Lanzerotti, E. N. Parker, Eds. (North-Holland, Amsterdam, 1978), vol. 2, pp. 321–402.
22. F. Bagenal and J. D. Sullivan, *J. Geophys. Res.* **86**, 8447 (1981).
23. E. C. Sittler, J. D. Scudder, H. S. Bridge, *Nature (London)* **292**, 711 (1981).
24. A. L. Broadfoot *et al.*, *Science* **212**, 206 (1981).
25. N. F. Ness, M. H. Acuña, K. W. Behannon, L. F. Burlaga, J. E. P. Connerney, R. P. Lepping, F. M. Neubauer, *ibid.* **215**, 558 (1982).

26. This report summarizes the work of many individuals who contributed their special talents in support of the Voyager 2 Saturn encounter. We are deeply indebted to them. We especially thank E. J. Franzgrote, O. Divers, R. Parker, and M. Fong at the Jet Propulsion Laboratory for their assistance in encounter planning and operations; J. Boughan, A. Bowes, J. Binsack, G. Gordon, Jr., P. Milligan, M. Terkoski, and S. Skinner at the Massachusetts Institute of Technology; P. Harrison of Computer Science Corporation; W. Mish and T. Carleton at the Goddard Space Flight Center for their support of the data reduction and analysis efforts. This work was sponsored by the National Aeronautics and Space Administration and performed under contract 953733 to the Jet Propulsion Laboratory.

* On leave from the Department of Geophysics and Planetary Science, Tel-Aviv University, Ramal-Aviv, Israel.

† Also at the Max-Planck-Institut für Aeronomie, Katlenburg-Lindau, West Germany.

10 November 1981